

## Inhibitory Effects of Dioscorea Polysaccharide on TNF- $\alpha$ -Induced Insulin Resistance in Mouse FL83B Cells

Bao-Hong Lee, Wei-Hsuan Hsu, and Tzu-Ming Pan\*

Department of Biochemical Science and Technology, College of Life Science, National Taiwan University, No. 1, Sec. 4, Roosevelt Road, Taipei 10617, Taiwan

**ABSTRACT:** *Dioscorea* is a traditional medicinal food in Asia. This study investigated the anti-insulin resistance of dioscorea polysaccharide (DPS) in inflammatory factor (tumor necrosis factor- $\alpha$ ; TNF- $\alpha$ ) induced mouse normal liver FL83B cells. Insulin resistance was induced by treating cells with TNF- $\alpha$  (20 ng/mL) for 5 h; subsequently, the medium was replaced with insulin and DPS for 60 min of incubation (model 1; alleviating group). In addition, cells were cotreated with TNF- $\alpha$  and DPS for 5 h in model 2 (preventing group). DPS effectively increased glucose uptake and glucose transporter 2 (GLUT2) expression of insulin-resistant cells. Furthermore, DPS stimulated insulin receptor substrate (IRS) tyrosyl phosphorylation and increased p-Akt level to alleviate insulin resistance in models 1 and 2. Finally, the possible mechanism of DPS promoting insulin sensitivity in TNF- $\alpha$ -induced FL83B cells was investigated in this study. DPS may attenuate c-Jun N-terminal kinases (JNK) and insulin resistance caused by TNF- $\alpha$  induction; therefore, DPS also elevated the levels of p-IRS<sup>Tyr</sup> and p-Akt<sup>Ser</sup> to improve insulin sensitivity in the TNF- $\alpha$ -induced FL83B cells.

**KEYWORDS:** dioscorea polysaccharide (DPS), tumor necrosis factor- $\alpha$  (TNF- $\alpha$ ), mouse normal liver FL83B cells, insulin resistance, c-Jun N-terminal kinases (JNK)

### INTRODUCTION

Type 2 diabetes (T2-D) is a chronic disease associated with carbohydrate metabolism and caused by a deficiency in insulin secretion or ineffectual insulin action. Medicinal plants constitute a common alternative treatment for T2-D in many parts of the world. Insulin resistance is associated with inflammatory factors such as tumor necrosis factor- $\alpha$  (TNF- $\alpha$ ) and interleukin-6 (IL-6) in T2-D patients. An association between the chronic activation of proinflammatory signaling pathways and loss of insulin sensitivity has been reported, and the TNF- $\alpha$ -mediated induction of insulin resistance in cell lines has been used as an in vitro model for antidiabetic investigations.<sup>1</sup> Cytokines are involved in the development of insulin resistance. The negative effect of TNF- $\alpha$  on insulin action is mediated by inhibiting the insulin signaling pathway.

TNF- $\alpha$  impairs insulin-dependent signal transduction through a mechanism that involves down-regulations of insulin receptor (IR) and insulin receptor substrate (IRS) and inhibition of tyrosine phosphorylation of IR and IRS increase serine (Ser)/threonine (Thr) phosphorylation of IRS to decrease the insulin-dependent pathway; furthermore, protein tyrosine (Tyr) phosphatase 1B (PTP1B) inhibition of glucose transporter (GLUT) expression through decreasing IRS<sup>Tyr</sup> phosphorylation has been reported.<sup>2</sup> Certain polysaccharides that are widely distributed in the plant kingdom may prevent the occurrence of oxidative stress and hyperglycemia in diabetic rats, including several polysaccharides obtained from green tea,<sup>3</sup> *Ganoderma lucidum*,<sup>4</sup> *Achyranthes bidentata*,<sup>5</sup> *Opuntia monacantha* cladode,<sup>6</sup> *Solanum lycocarpum* fruits,<sup>7</sup> and *Lycium barbarum*.<sup>8</sup> Astragalus polysaccharides were found to decrease the expression of PTP1B by relieving endoplasmic reticulum (ER) stress in type 2 diabetic rats.<sup>9</sup>

Steroidal saponin was identified as the major active compound responsible for the antihyperglycemic effect of yam.<sup>10,11</sup>

Furthermore, the immunomodulatory protein, dioscorin, has been identified from yam and investigated in a recent study.<sup>12</sup> Dioscorealide B was purified from yam and reported to possess anti-inflammatory activity and inhibit nitric oxide production.<sup>13</sup> In previous studies, yam (*Dioscorea batatas*) was reported to have a regulatory effect on blood glucose and antidiabetic activity in rats exposed to high-fructose diets.<sup>14,15</sup> These results indicate that yam has antidiabetic capacities; however, the effect of yam polysaccharides on decreasing insulin resistance is unclear. The aim of the present study was to investigate the promotion of an insulin-sensitive effect of yam polysaccharides in insulin-resistant FL83B cells.

### MATERIALS AND METHODS

**Materials and Chemicals.** 3-(4,5-Dimethylthiazol-2-yl)-2,5-diphenyltetrazolium bromide (MTT), fetal bovine serum (FBS), Triton-X 100, and trypsin were purchased from Sigma Co. (St. Louis, MO). F12-K medium, sodium bicarbonate, penicillin, and streptomycin were purchased from HyClone Laboratories (Logan, UT). 2-[N-(7-Nitrobenz-2-oxa-1,3-diazol-4-yl) amino]-2-deoxy-D-glucose (2-NBDG) and nicotinamide adenine dinucleotide phosphate (NADPH) assay kits were from Invitrogen (Carlsbad, CA). The Bio-Rad protein assay dye was from Bio-Rad Laboratories (Hercules, CA). Mouse tumor necrosis factor alpha (TNF- $\alpha$ ) was obtained from Preprotech (London, U.K.).

**Plant Material and Dioscorea Polysaccharide (DPS) Preparation.** Approximately 25 g of dioscorea root (*D. batatas* Dence) powder (purchased from a local market, Taipei, Taiwan) was mixed with 250 mL of deionized water, and the crude polysaccharides were

**Received:** December 6, 2010

**Revised:** April 9, 2011

**Accepted:** April 10, 2011

**Published:** April 11, 2011

extracted at 95 °C for 30 min. After extraction, the aqueous extract was concentrated at vacuum, and then the crude DPS was obtained by 95% ethanol precipitation, washed, filtered, and freeze-dried. Moreover, the yield of DPS is 37.2%, and the DPS was stored at -20 °C until used.

**Total Carbohydrate and Crude Protein Assays.** The total carbohydrate level of DPS was measured by using the phenol-sulfuric acid method.<sup>16</sup> The crude protein level of DPS was assayed by using a Bio-Rad protein assay dye.

**Cell Culture.** The FL83B cell line is a mouse normal liver cell from the Bioresource Collection and Research Center (BCRC) in Taiwan (Hsinchu, Taiwan), which is cultured in the F12-K medium supplemented with 10% heat-inactivated FBS and antibiotics (100 units/mL penicillin and 100 µg/mL streptomycin). Cells were cultured at 37 °C in a humidified atmosphere of 5% CO<sub>2</sub>.

**Assay for DPS by High-Performance Anion Exchange Chromatography (HPAEC)**<sup>17</sup>. DPS was hydrolyzed using 1 mL of trifluoroacetic acid (TFA; 2 M) for 2 h at 100 °C and dried, respectively. The hydrolytic products were washed with methanol and dried using a centrifugal vacuum evaporator (ThermoQuest, Hampshire, U.K.). The dry residue was resuspended in deionized water. The analysis of monosaccharides in DPS was carried out on an HPAEC system (Dionex, Sunnyvale, CA) equipped with a quaternary GP40 gradient pump (Dionex) and an ED40 conductivity detector (Dionex). The analytical column used a CarboPac PA1 (4 mm × 250 mm i.d., 5 µm, Dionex) and a guard column (4 mm × 50 mm). Elution was carried out at a flow rate of 1.0 mL/min at 37 °C for 60 min. Mobile phase A was 8.75 mM Ba(OH)<sub>2</sub>, and mobile phase B consisted of 2 mM Ba(OH)<sub>2</sub>, 100 mM NaOH, and 100 mM NaOAc, respectively. A gradient elution of 100–100% by mobile phase A and mobile phase B was performed for 0–30–60 min.

**Cell Viability.** Mouse FL83B cells (1.5 × 10<sup>4</sup> cells per well) were seeded into 24-well plates overnight. Cells were treated with TNF-α (20 ng/mL) and DPS (50–300 µg/mL) in serum-free F12-K medium for 5 h. Subsequently, cells were washed with phosphate-buffered saline (PBS) twice, and 1 mL of medium containing MTT (0.5 mg/mL) was added to react for 2 h at 37 °C. After reaction, serum-free medium was removed, and cells were washed with PBS; the MTT reacted product (formazan crystals) was dissolved in 0.5 mL of dimethyl sulfoxide (DMSO), and the absorption was measured at 570 nm by an ELISA reader for cell viability assay. Furthermore, cell viability was also evaluated by crystal violet stain. Cells were seeded on 24-well plates (1.5 × 10<sup>4</sup> cells/well) and treated with TNF-α (20 ng/mL) and various concentrations of DPS for 5 h. The medium was then removed, washed with PBS, and stained with 2 g/L crystal violet for 20 min before being washed with deionized water. Crystal violet was dissolved in 20 g/L SDS solution and measured at 600 nm.

**Insulin Resistance Induction and Glucose (2-NBDG) Uptake.** The insulin sensitivity of FL83B cells was evaluated by two models. Glucose uptake of FL83B cells was assessed using the fluorescent glucose analogue, 2-NBDG. The FL83B cells were seeded in 10 cm dishes at a density of 5 × 10<sup>5</sup>/well, and grown until 80% confluence was reached.<sup>1</sup> In model 1 (alleviating group), cells were induced with insulin resistance by treatment with TNF-α (20 ng/mL final concentration) dissolved in serum-free F12-K medium for 5 h; subsequently, the medium was removed and replaced with Krebs-Ringer-bicarbonate (KRB) buffer containing DPS (50–200 µg/mL final concentration), insulin (500 nM final concentration), and 2-NBDG (160 µM final concentration) for 60 min of incubation. Moreover, cells of model 2 (preventing group) were treated with TNF-α (20 ng/mL final concentration) and DPS (50–200 µg/mL final concentration) dissolved in serum-free F12-K medium for 5 h of incubation. After incubation, the medium was replaced with KRB buffer containing insulin (500 nM final concentration) and 2-NBDG (160 µM final concentration) for 60 min. Subsequently, the glucose uptake activity of

FL83B cells was determined with a FACS flow cytometer (Becton Dickinson, San Jose, CA) and analyzed using CellQuest software. The background of 2-NBDG fluorescence was deduced.

**Western Blot Analysis.** FL83B cells were lysed in ice-cold lysis buffer containing 20 mM Tris-HCl (pH 7.4), 1% of Triton X-100, 0.1% of SDS, 2 mM EDTA, 10 mM NaF, 1 mM phenylmethanesulfonyl fluoride (PMSF), 500 µM sodium vanadate, and 10 µg/mL aprotinin overnight. Then the cell lysates were sonicated with ice cooling (four times, each 15 s) and then centrifuged (12000g, 10 min) to recover the supernatant. The supernatant was taken as the cell extract. The protein concentration in the cell extract was determined using a Bio-Rad protein assay kit. The samples were subjected to 10% sodium dodecyl sulfate-polyacrylamide gel electrophoresis (SDS-PAGE). The protein spots were electrotransferred to a polyvinylidene difluoride (PVDF) membrane. The membrane was incubated with block buffer (PBS containing 0.05% of Tween 20 and 5% w/v nonfat dry milk) for 1 h, washed with PBS containing 0.05% Tween 20 (PBS-T) three times, and then probed with a 1:1000 diluted solution of anti-Akt antibody and 1:1000 diluted solution of anti-p-Akt, anti-p-IRS (1:2000), anti-p-IR (1:5000), anti-JNK (1:1000), anti-p-JNK (1:1000), and anti-GLUT-2 (1:1000) antibodies (Cell Signaling Technology, Beverly, MA) overnight at 4 °C. In addition, the intensity of the blots probed with the 1:1000 diluted solution of mouse monoclonal antibody to bind GAPDH (Cell Signaling Technology) was used as the control to ensure that a constant amount of protein was loaded into each lane of the gel. The membrane was washed three times each for 5 min in PBS-T, shaken in a solution of HRP-linked anti-rabbit IgG secondary antibody, and washed three more times each for 5 min in PBS-T. The expressions of protein were detected by enhanced chemiluminescent (ECL) reagent (Millipore, Billerica, MA).

**Statistical Analysis.** Experimental results were averaged triplicate analyses. The data were recorded as the mean ± standard deviation (SD) and analysis by statistical analysis system (SAS Inc., Cary, NC). One-way analysis of variance was performed by ANOVA procedures. Significant differences between means were determined by Duncan's multiple-range tests. Results were considered to be statistically significant at  $p < 0.05$ .

## RESULTS

**HPAEC Assay for DPS Contents.** The DPS compositions were analyzed by HPAEC. Through comparison of the retention time with standards, the monosaccharide composition in DPS (0.1 mg/mL) was identified (Figure 1). Monosaccharides, disaccharides, including fructose (Fru), arabinose (Ara), galactose (Gal), glucose (Glc), mannose (Man), and maltose (Mal), total carbohydrate, and crude protein were quantified (Table 1). The relative concentrations of Ara, Glc, Gal, Man, and Mal were 0.017, 0.781, 0.083, 0.049, and 0.041 mM in the DPS, respectively. Furthermore, the total carbohydrate and crude protein contents of DPS were 9998.6 mg/g and 13.2 µg/g, respectively, suggesting a highly pure DPS was obtained in this study.

**Cytotoxicity and Induction of Insulin Resistance.** The ability of TNF-α to induce insulin resistance in FL83B cells has been demonstrated previously.<sup>18–20</sup> However, on the basis of the activity of TNF-α as one of the inflammatory factors affecting cell viability, apoptosis, and proliferation, thereby the cytotoxicity of DPS and TNF-α was evaluated in this study.

The FL83B cell line was used as a cell model for treatment with TNF-α (20 ng/mL) and DPS (50, 100, 200, and 300 µg/mL) for 5 h, and the cell viability was evaluated by the MTT assay. MTT, a yellow tetrazole, is reduced to purple formazan in living cells by mitochondrial reductase. Treatment with TNF-α (20 ng/mL)

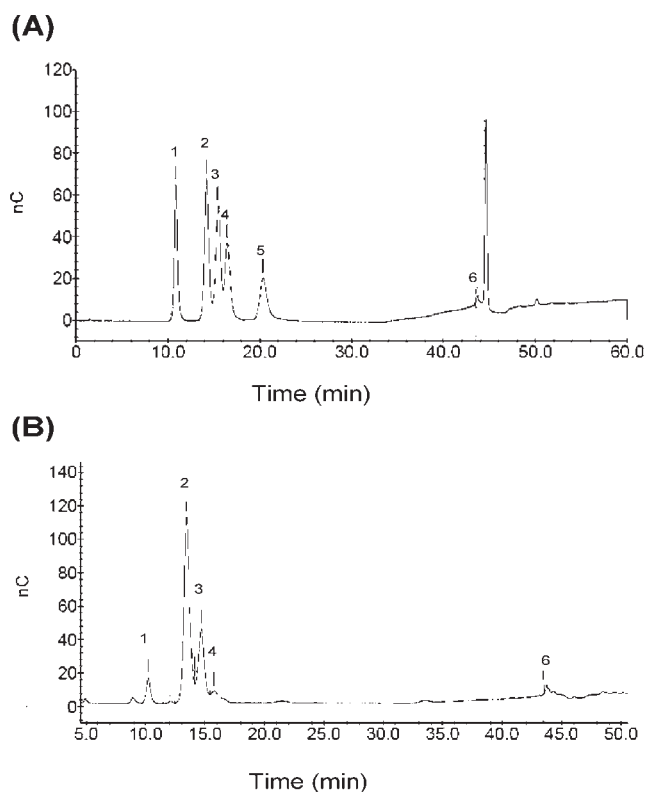


**Figure 1.** High-performance anion exchange chromatography (HPAEC) graph of standard (A) and DPS (B). Peaks: (1) Ara, (2) Glc, (3) Gal, (4) Man, (5) Fru, and (6) Mal.

**Table 1.** Components of DPS<sup>a</sup>

monosaccharides and disaccharides (mM)	total carbohydrate (mg/g)	crude protein ( $\mu\text{g/g}$ )
Ara	0.017 $\pm$ 0.003	
Glc	0.781 $\pm$ 0.008	
Gal	0.083 $\pm$ 0.001	9998.6 $\pm$ 14.8
Man	0.049 $\pm$ 0.004	13.2 $\pm$ 0.1
Mal	0.041 $\pm$ 0.002	

<sup>a</sup>The analysis of monosaccharides and disaccharides of DPS was carried out on an HPAEC system. The injection concentration of DPS was 0.

and DPS (300  $\mu\text{g/mL}$ ) significantly resulted in cytotoxicity in the FL83B cell; however, treatment with DPS (100 and 200  $\mu\text{g/mL}$ ) for 5 h increased living cells (Figure 2A). This result may be because of DPS interference in MTT and mitochondrial enzyme activity. Therefore, we chose crystal violet stain to confirm the cytotoxicity of DPS for the 5 h treatment. The results indicated that DPS (50–200  $\mu\text{g/mL}$ ) did not display cytotoxicity for FL83B cells for 5 h of treatment (Figure 2B).

Subsequently, the optimal condition for insulin resistance induction was investigated, and the glucose uptake activity of insulin-resistant FL83B cells was evaluated by 2-NBDG assay. The fluorescent glucose analogue, 2-NBDG, is a D-glucose fluorescent derivative and optimally measured glucose uptake activity of cells other than D-glucose. Insulin-resistant cells were treated with 500 nM insulin for 15, 30, 45, 60, 75, and 90 min, respectively. Results indicated that treatment of FL83B cells with 20 ng/mL of TNF- $\alpha$  for 5 h triggered a significant decrease in 2-NBDG uptake compared to the control group at 45 and 60 min

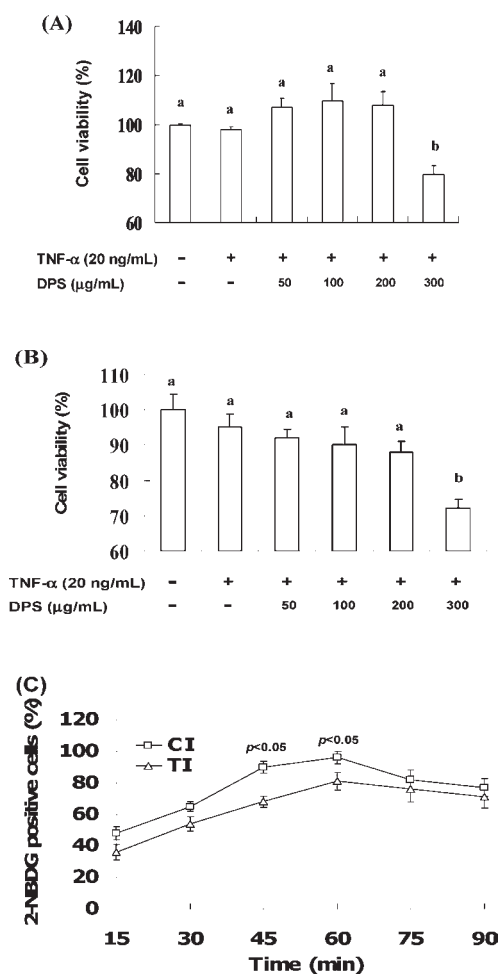


**Figure 2.** Effects of TNF- $\alpha$  and DPS (5 h treatment) on the cell viability by MTT stain (A) and crystal violet stain (B). Insulin resistance was induced and evaluated by 2-NBDG uptake activity of mouse normal liver FL83B cell line (C). Cells were treated with TNF- $\alpha$  (20 ng/mL) for 5 h and then incubated with insulin (500 nM) for 15, 30, 45, 60, 75, and 90 min, respectively. TI, TNF- $\alpha$  + insulin; CI, control + insulin. Different letters indicate statistically significant differences ( $p < 0.05$ ).

(Figure 2C), suggesting the incubation time of 2-NBDG is the optimal treated condition. Therefore, 60 min of incubation of 2-NBDG was chosen in this study. Taken together, these results confirmed that the cytokine TNF- $\alpha$  is a mediator of insulin resistance. Incubation with TNF- $\alpha$  (20 ng/mL) was therefore shown to be an effective treatment to prepare insulin-resistant FL83B cells.

**2-NBDG Uptake Activity in Insulin-Resistant Cells Treated with DPS.** The effect of DPS on glucose uptake activity in the FL83B cells was investigated by two models. Insulin resistance was induced by TNF- $\alpha$  (20 ng/mL) treatment for 5 h, followed by stimulation with insulin and DPS for 60 min (model 1). In model 2, cells were cotreated with TNF- $\alpha$  (20 ng/mL) and DPS (50, 100, and 200  $\mu\text{g/mL}$ ) for 5 h, and then cells were stimulated with 500 nM insulin for 60 min. After incubation, the 2-NBDG uptake activity of FL83B cells was determined by FACS. As shown in Figure 3A,B, treatment of DPS (200  $\mu\text{g/mL}$ ) significantly recovered 2-NBDG uptake, thus alleviating TNF- $\alpha$ -induced insulin resistance in model 1. DPS also increased the mean fluorescent intensity of 2-NBDG in FL83B cells. In addition,



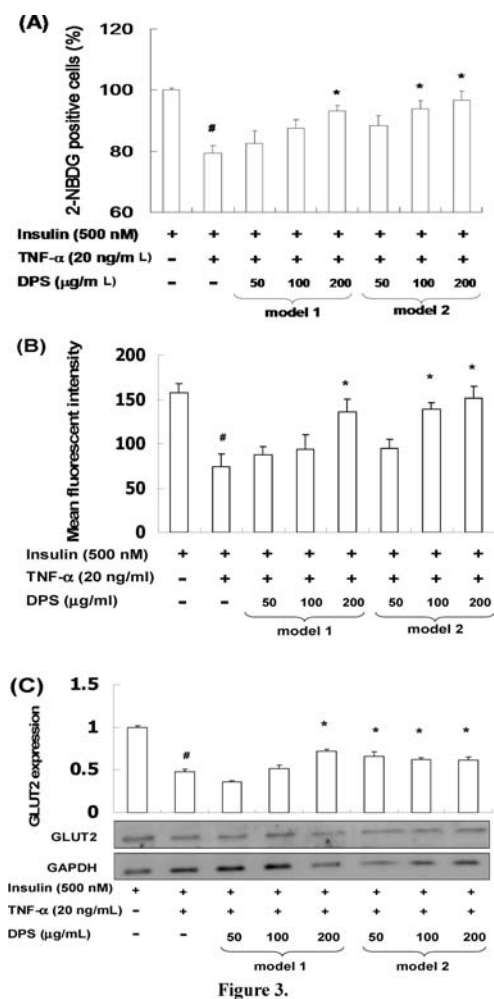
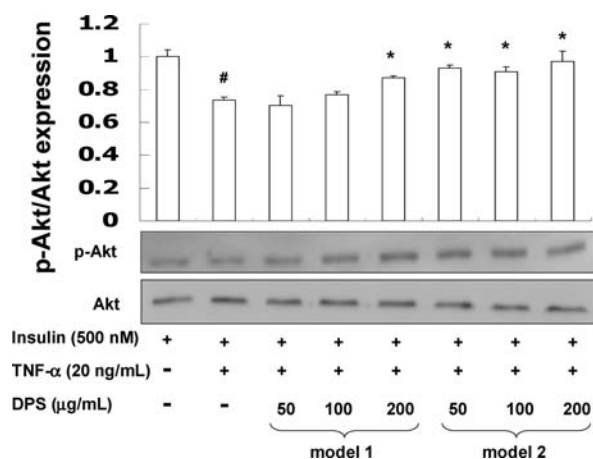


Figure 3.

**Figure 3.** Improvement effect of DPS on insulin-resistant FL83B cells: 2-NBDG uptake activity (A); mean fluorescent intensity of 2-NBDG in FL83B cells (B); GLUT2 expression of FL83B cells treated with DPS (C). Model 1: FL83B cells were induced with insulin resistance by TNF- $\alpha$  (20 ng/mL) inducing for 5 h and then treating with different doses of DPS (50, 100, and 200  $\mu$ g/mL) and insulin (500 nM) for 1 h. Model 2: FL83B cells were treated with TNF- $\alpha$  and DPS for 5 h and then incubated with insulin for 1 h. #, significantly different ( $p < 0.05$ ) from the control + insulin (CI) group; \*, significantly different ( $p < 0.05$ ) from the TNF- $\alpha$  + insulin (TI) group.

DPS (100 and 200  $\mu$ g/mL) inhibited TNF- $\alpha$ -induced insulin resistance, increasing the 2-NBDG uptake activity of cells and the mean fluorescent intensity of 2-NBDG in model 2.

**GLUT-2 Expression in Insulin-Resistant Cells.** GLUT-2 is a transporter protein that regulates glucose uptake. GLUT-2 is found at high levels in the liver, small intestine, kidney, and pancreatic  $\beta$ -cells and plays a role in mediating both glucose influx and efflux in hepatocytes. Inhibition of GLUT-2 expression by TNF- $\alpha$  treatment has been reported by Feinstein et al.<sup>21</sup> In the present study, treatment with DPS (50, 100, and 200  $\mu$ g/mL) prevented the decrease in GLUT-2 expression caused by TNF- $\alpha$ , leading to an increase in 2-NBDG uptake in model 2. Similarly, treatment with DPS at 200  $\mu$ g/mL effectively promoted insulin sensitivity in insulin-resistant FL83B cells by stimulating GLUT2 expression (model 1) (Figure 3C), suggesting that DPS induced the GLUT2-mediated recovery of insulin sensitivity in TNF- $\alpha$ -treated FL83B cells.



**Figure 4.** Improvement effect of DPS on p-Akt and Akt expressions of FL83B cells. Model 1: FL83B cells were induced with insulin resistance by TNF- $\alpha$  (20 ng/mL) inducing for 5 h and then treating with different doses of DPS (50, 100, and 200  $\mu$ g/mL) and insulin (500 nM) for 1 h. Model 2: FL83B cells were treated with TNF- $\alpha$  and DPS for 5 h and then incubated with insulin for 1 h. #, significantly different ( $p < 0.05$ ) from the control + insulin (CI) group; \*, significantly different ( $p < 0.05$ ) from the TNF- $\alpha$  + insulin (TI) group.

**Effect of DPS Treatment on Akt and p-Akt Expression in Insulin-Resistant Cells.** Akt is the key molecule that mediates the metabolic effects of insulin signaling. Akt is downstream of phosphatidylinositol 3 kinase (PI3K) and facilitates glucose uptake and glycogen synthesis in the liver. Akt is phosphorylated at Ser473 by PI3K via insulin stimulation to form active p-Akt.<sup>21</sup> The present results (Figure 4) clearly demonstrated that TNF- $\alpha$  treatment (20 ng/mL; 5 h) inhibited Akt phosphorylation compared to the control group. However, the inhibition of Akt phosphorylation by TNF- $\alpha$  was inhibited and improved by treatment with DPS in models 1 and 2.

**p-IR and p-IRS Expression in Insulin-Resistant Cells.** IR is a heterotetrameric membrane glycoprotein consisting of two  $\alpha$ -subunits and two  $\beta$ -subunits. When insulin binds to the  $\alpha$ -subunit of IR, the intracellular  $\beta$ -subunit becomes activated by phosphorylation of specific Tyr residues, which in turn causes binding and activation (Tyr phosphorylation) of IRS protein, which is the most important receptor substrate in cells that respond to insulin with Akt phosphorylation and GLUT translocation. This mechanism appears to be important in the etiology of insulin resistance in human type 2 diabetes. TNF- $\alpha$  treatment is reported to decrease the protein expression of IR and inhibits the tyrosyl phosphorylation of IR in insulin-stimulated 3T3-L1 and myeloid 32D cells.<sup>21</sup> In the present study, the p-IR (Tyr1146) level was significantly decreased in the TNF- $\alpha$  inducing group and was not recovered by DPS treatment (Figure 5A). However, DPS (200  $\mu$ g/mL) significantly elevated the p-IRS (Tyr896) level to stimulate insulin sensitivity in models 1 and 2 (Figure 5B). These may be an insulin-stimulated insulin signaling pathway by IR and IRS phosphorylation, but phosphorylation of IR was not maintained after insulin stimulation for 1 h, nor that of IRS.

**Inhibitory Effect of JNK Phosphorylation by DPS.** IRS is a target of protein kinase C (PKC) and c-Jun N-terminal kinase (JNK) for Ser/Thr phosphorylation caused by high glucose and TNF- $\alpha$ .<sup>22,23</sup> The JNK signaling cascade is one of the pro-inflammatory pathways involved in JNK phosphorylation. Inflammatory cytokines can induce p-JNK activation, and p-JNK

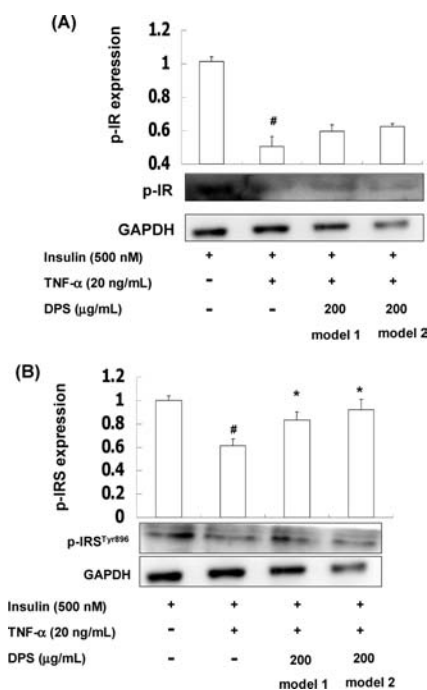


**Figure 5.** Improvement effect of DPS on p-IR (A) and p-IRS (B) levels of FL83B cells. Model 1: FL83B cells were induced with insulin resistance by TNF- $\alpha$  (20 ng/mL) inducing for 5 h and then treating with different doses of DPS (50, 100, and 200  $\mu$ g/mL) and insulin (500 nM) for 1 h. Model 2: FL83B cells were treated with TNF- $\alpha$  and DPS for 5 h and then incubated with insulin for 1 h. #, significantly different ( $p < 0.05$ ) from the control + insulin (CI) group; \*, significantly different ( $p < 0.05$ ) from the TNF- $\alpha$  + insulin (TI) group.

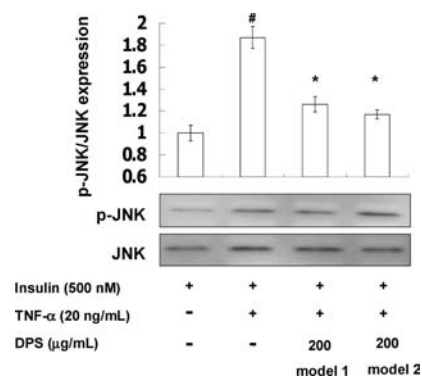


**Figure 6.** Inhibitory effect of DPS on JNK phosphorylation in FL83B cells. Model 1: FL83B cells were induced with insulin resistance by TNF- $\alpha$  (20 ng/mL) inducing for 5 h and then treating with different doses of DPS (50, 100, and 200  $\mu$ g/mL) and insulin (500 nM) for 1 h. Model 2: FL83B cells were treated with TNF- $\alpha$  and DPS for 5 h and then incubated with insulin for 1 h. #, significantly different ( $p < 0.05$ ) from the control + insulin (CI) group; \*, significantly different ( $p < 0.05$ ) from the TNF- $\alpha$  + insulin (TI) group.

can inhibit IRS attenuating the insulin signaling pathway (Akt/PKB) through Ser/Thr phosphorylation, resulting in insulin resistance. Results demonstrated that DPS (200  $\mu$ g/mL) significantly decreased the level of p-JNK/JNK in TNF- $\alpha$ , inducing insulin-resistant FL83B cells (in models 1 and 2), suggesting an increase in insulin sensitivity by DPS treatment via inhibitory effect of JNK phosphorylation (Figure 6).

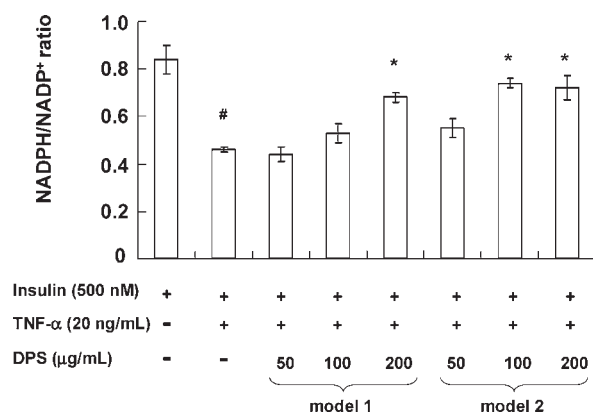


**Figure 7.** Antioxidative effect of DPS on NADPH/NADP<sup>+</sup> level. Model 1: FL83B cells were induced with insulin resistance by TNF- $\alpha$  (20 ng/mL) inducing for 5 h and then treating with different doses of DPS (50, 100, and 200  $\mu$ g/mL) and insulin (500 nM) for 1 h. Model 2: FL83B cells were treated with TNF- $\alpha$  and DPS for 5 h and then incubated with insulin for 1 h. #, significantly different ( $p < 0.05$ ) from the control + insulin (CI) group; \*, significantly different ( $p < 0.05$ ) from the TNF- $\alpha$  + insulin (TI) group.

**NADPH/NADP<sup>+</sup> Ratio in Insulin-Resistant Cells.** Inflammation is always associated with oxidative stress, and the NADPH level is one of the markers of antioxidative capacity. In models 1 and 2, DPS treatment effectively elevated NADPH levels in FL83B cells in comparison to the TNF- $\alpha$ -induced group (Figure 7). This result may be due to the DPS-induced increase in glucose metabolism, which could result in an activation of the pentose phosphate pathway and an increase in NADPH synthesis.

## DISCUSSION

Hyperglycemia is a deficiency in the hepatic control of glucose homeostasis. The impairment of insulin ability to trigger downstream metabolic actions in the liver is defined as hepatic insulin resistance.<sup>24</sup> Recent studies have explained that functions of IRS, which is one family of docking molecules connecting IR activation to essential downstream kinase cascades, are the key molecular lesions causing hepatic insulin resistance.<sup>25,26</sup> Ser/Thr phosphorylation of IRS attenuates the insulin-stimulating activities of PI3K and Akt because Ser/Thr phosphorylation affects IRS phosphorylation at tyrosine residues.<sup>27</sup>

Previous studies demonstrated IRS as a target of kinase such as c-Jun N-terminal kinase (JNK), and high glucose and inflammatory factors are also known to activate kinase.<sup>22,23</sup> Activation of JNK induces Ser307 phosphorylation of IRS, which blocks the downstream activation of the Akt pathway. Reactive oxygen species (ROS) are chemically reactive molecules containing oxygen (oxygen ions and peroxides), and ROS accumulates into a situation known as oxidative stress. ROS have been suggested as upstream regulators of Ser/Thr kinase under high-glucose conditions.<sup>28</sup> Preventing activation of Ser/Thr kinase against high-glucose-induced Ser/Thr phosphorylation of IRS has been reported.<sup>29</sup> In addition, the effect of certain clinical insulin-sensitizing drugs such as rosiglitazone reducing high-glucose-induced toxicity by inhibiting Ser/Thr kinase is well-known.<sup>30</sup>

Several studies have reported that polysaccharides from *Astragalus membranaceus* (astragalus) inhibit PTP1B and endoplasmic reticulum (ER) stress-induced insulin resistance and increase Akt/PKB signaling pathway activity and GLUT4

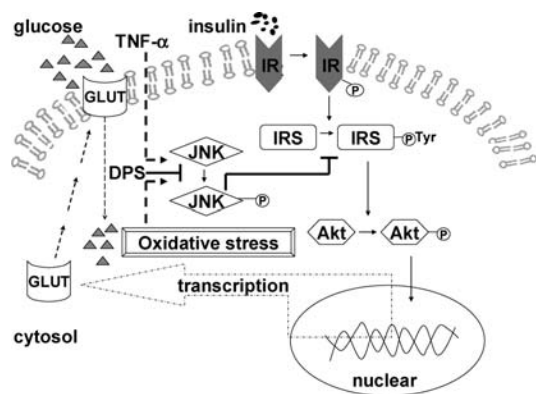


**Figure 8.** Insulin resistance-alleviating mechanism by DPS treatment in FL83B cells. TNF- $\alpha$ -induced JNK phosphorylation was inhibited by DPS treatment in models 1 and 2, improving GLUT2 expression and 2-NBDG uptake.

expression in skeletal muscle.<sup>9,31</sup> Furthermore, the antioxidative activity of *G. lucidum*, *A. bidentata*, *O. monacantha*, *S. lycocarpum* fruits, and *L. barbarum* polysaccharides has been reported in diabetic rats.<sup>4–8</sup> Moreover, the association between a hypoglycemic effect and the structural features of *Cynomorium songaricum* polysaccharides has been investigated in the STZ-induced diabetic rat.<sup>32</sup> These studies demonstrated that polysaccharides derived from plants or fungi may improve insulin sensitivity in vivo and in vitro. Many researchers have indicated that dioscorea improves glucose metabolism and insulin resistance in rats,<sup>14,15</sup> and active compounds identified from dioscorea and showing antidiabetic activity in STZ-induced rats have been demonstrated.<sup>10,11</sup> However, the effect of dioscorea polysaccharides on insulin resistance remains unclear.

On the other hand, an association between oxidative stress and insulin resistance has been reported in diabetes.<sup>33</sup> In the oxidative stage of the pentose phosphate pathway, glucose-6-phosphate is converted to NADPH and ribose-5-phosphate by glucose-6-phosphate dehydrogenase, resulting in an increase in NADPH (reducing agent) further to inhibiting oxidative stress. In the present study, an increase of NADPH was found by DPS treatment to prevent TNF- $\alpha$ -induced insulin resistance in cells.

We therefore hypothesized that DPS may inhibit TNF- $\alpha$ -induced insulin resistance through the activation of JNK. In keeping with this observation, DPS inhibits an elevation in JNK activity from an inflammatory factor, resulting in an increase in IRS<sup>Tyr</sup> phosphorylation and improving the insulin signal pathway.<sup>34</sup> The results suggested that DPS elevated the levels of p-IR and p-Akt, there by improving insulin sensitivity in the TNF- $\alpha$ -induced FL83B cell models 1 and 2 (Figure 8).

## AUTHOR INFORMATION

### Corresponding Author

\*Phone: +886-2-33664519, ext 10. Fax: +886-2-33663838. E-mail: tmpan@ntu.edu.tw.

## ACKNOWLEDGMENT

We thank Editage Pvt. Ltd. for providing language help.

## REFERENCES

(1) Huang, D. W.; Shen, S. C.; Wu, J. S. B. Effects of caffeic acid and cinnamic acid on glucose uptake in insulin-resistant mouse hepatocytes. *J. Agric. Food Chem.* **2009**, *57*, 7687–7692.

(2) Cheung, A. T.; Wang, J.; Ree, D.; Kolls, J. K.; Bryer-Ash, M. Tumor necrosis factor-R induces hepatic insulin resistance in obese Zucker (fa/fa) rats via interaction of leukocyte antigen-related tyrosine phosphatase with focal adhesion kinase. *Diabetes* **2000**, *49*, 810–819.

(3) Chen, X. Q.; Lin, Z.; Ye, Y.; Zhang, R.; Yin, J. F.; Jiang, Y. W.; Wang, H. T. Suppression of diabetes in non-obese diabetic (NOD) mice by oral administration of water-soluble and alkali-soluble polysaccharide conjugates prepared from green tea. *Carbohydr. Polymer* **2010**, *82*, 28–33.

(4) Jia, J.; Zhang, X.; Hu, Y. S.; Wu, Y.; Wang, Q. Z.; Li, N. N.; Guo, Q. C.; Dong, X. C. Evaluation of in vivo antioxidant activities of *Ganoderma lucidum* polysaccharides in STZ-diabetic rats. *Food Chem.* **2009**, *115*, 32–36.

(5) Xue, S. X.; Chen, X. M.; Lu, J. X.; Jin, L. Q. Protective effect of sulfated *Achyranthes bidentata* polysaccharides on streptozotocin-induced oxidative stress in rats. *Carbohydr. Polymer* **2009**, *75*, 415–419.

(6) Yang, N.; Zhao, M. M.; Zhu, B. H.; Yang, B.; Chen, C. H.; Cui, C.; Jiang, Y. M. Anti-diabetic effects of polysaccharides from *Opuntia monacantha* cladode in normal and streptozotocin-induced diabetic rats. *Innovative Food Sci. Emerging Technol.* **2008**, *9*, 570–574.

(7) Dall'Agno, R.; Von Poser, G. L. The use of complex polysaccharides in the management of metabolic diseases: the case of *Solanum lycocarpum* fruits. *J. Ethnopharmacol.* **2000**, *71*, 337–341.

(8) Li, M. M. Protective effect of *Lycium barbarum* polysaccharides on streptozotocin-induced oxidative stress in rats. *Int. J. Biol. Macromol.* **2007**, *40*, 461–465.

(9) Wang, N.; Zhang, D. L.; Mao, X. Q.; Zou, F.; Jin, H.; Ouyang, J. P. Astragalus polysaccharides decreased the expression of PTP1B through relieving ER stress induced activation of ATF6 in a rat model of type 2 diabetes. *Mol. Cell. Endocrinol.* **2009**, *307*, 89–98.

(10) McAnuff, M. A.; Harding, W. W.; Omoruyi, F. O.; Jacobs, H.; Morrison, E. Y.; Asemota, H. N. Hypoglycemic effects of steroidal sapogenins isolated from Jamaican bitter yam, *Dioscorea polygonoides*. *Food Chem. Toxicol.* **2005**, *43*, 1667–1672.

(11) McAnuff-Harding, M. A.; Omoruyi, F. O.; Asemota, H. N. Intestinal disaccharidases and some renal enzymes in streptozotocin-induced diabetic rats fed sapogenin extract from bitter yam (*Dioscorea polygonoides*). *Life Sci.* **2006**, *78*, 2595–2600.

(12) Liu, Y. W.; Shang, H. F.; Wang, C. K.; Hsu, F. L.; Hou, W. C. Immunomodulatory activity of dioscorin, the storage protein of yam (*Dioscorea alata* cv. Tainong No. 1) tuber. *Food Chem. Toxicol.* **2007**, *45*, 2312–2318.

(13) Hiransai, P.; Ratanachaiyavong, S.; Itharat, A.; Graidist, P.; Ruengrairatanaroj, P.; Purintrapiban, J. Dioscorealide B suppresses LPS-induced nitric oxide production and inflammatory cytokine expression in RAW 264.7 macrophages: the inhibition of NF- $\kappa$ B and ERK1/2 activation. *J. Cell. Biochem.* **2010**, *109*, 1057–1063.

(14) Hashimoto, N.; Noda, T.; Kim, S. J.; Sarkerm, M. Z. I.; Yamauchi, H.; Takigawa, S.; Matsuura-Endo, C.; Suzuki, T.; Han, K. H.; Fukushima, M. Yam contributes to improvement of glucose metabolism in rats. *Plant Foods Hum. Nutr.* **2009**, *64*, 193–198.

(15) Hsu, J. H.; Wu, Y. C.; Liu, I. M.; Cheng, J. T. Dioscorea as the principal herb of Die-Huang-Wan, a widely used herbal mixture in China, for improvement of insulin resistance in fructose-rich chow-fed rats. *J. Ethnopharmacol.* **2007**, *112*, 577–584.

(16) Xi, X. G.; Wei, X. L.; Wang, Y. F.; Chu, W. J.; Xiao, J. B. Determination of tea polysaccharides in *Camellia sinensis* by a modified phenol-sulfuric acid method. *Arch. Biol. Sci.* **2010**, *62*, 671–678.

(17) Iqbal, S.; Nguyen, T. H.; Nguyen, T. T.; Maischberger, T.; Haltrich, D.  $\beta$ -Galactosidase from *Lactobacillus plantarum* WCFS1: biochemical characterization and formation of prebiotic galacto-oligosaccharides. *Carbohydr. Res.* **2010**, *345*, 1408–1416.

(18) Cheng, H. L.; Huang, H. K.; Chang, C. I.; Tsai, C. P.; Chou, C. H. A cell-based screening identifies compounds from the stem of *Momordica charantia* that overcome insulin resistance and activate AMP activated protein kinase. *J. Agric. Food Chem.* **2008**, *56*, 6835–6843.

(19) Kim, S. K.; Kim, J. Y.; Lee, M. K.; Lee, B. W.; Lee, H. C.; Lee, E. J. Adual-reporter system for specific tracing of pancreatic  $\beta$ -cell lines



that non-invasively measures viable in vivo islet cells. *Biotechnol. Lett.* **2010**, *32*, 53–57.

(20) Shahid, G.; Hussain, T. GRK2 negatively regulates glycogen synthesis in mouse liver FL83B cells. *J. Biol. Chem.* **2007**, *282*, 20612–20620.

(21) Feinstein, R.; Kanety, H.; Papa, M. Z.; Lunenfeld, B.; Karasik, A. Tumor necrosis factor- $\alpha$  suppresses insulin-induced tyrosine phosphorylation of insulin receptor and its substrates. *J. Biol. Chem.* **1993**, *268*, 26055–26058.

(22) Mussig, K.; Staiger, H.; Fiedler, H.; Moeschel, K. Shp2 is required for protein kinase C-dependent phosphorylation of serine307 in insulin receptor substrate-1. *J. Biol. Chem.* **2005**, *280*, 32693–32699.

(23) Nakatani, Y.; Kaneto, H.; Kawamori, D.; Hatazaki, M. Modulation of the JNK pathway in liver affects insulin resistance status. *J. Biol. Chem.* **2004**, *279*, 45803–45809.

(24) Kim, S. P.; Ellmerer, M.; Can Citters, G. W.; Bergman, R. N. Primacy of hepatic insulin resistance in the development of the metabolic syndrome induced by an isocaloric moderate-fat diet in the dog. *Diabetes* **2003**, *52*, 2453–2460.

(25) Thirone, A. C.; Huang, C.; Klip, A. Tissue-specific roles of IRS proteins in insulin signaling and glucose transport. *Trends Endocrinol. Metab.* **2006**, *17*, 72–78.

(26) Petersen, K. F.; Shulman, G. L. Etiology of insulin resistance. *Am. J. Med.* **2006**, *119*, S10–S16.

(27) Hartman, M. E.; Villela-Bach, M.; Chen, J.; Freund, G. G. Frap-dependent serine phosphorylation of IRS-1 inhibits IRS-1 tyrosine phosphorylation. *Biochem. Biophys. Res. Commun.* **2001**, *280*, 776–781.

(28) Lee, H. B.; Yu, M. R.; Song, J. S.; Ha, H. Reactive oxygen species amplify protein kinase C signaling in high glucose-induced fibronectin expression by human peritoneal mesothelial cells. *Kidney Int.* **2004**, *65*, 1170–1179.

(29) Idris, I.; Gray, S.; Donnelly, R. Protein kinase C activation: isozyme-specific effects on metabolism and cardiovascular complications in diabetes. *Diabetologia* **2001**, *44*, 659–673.

(30) Hwang, J. T.; Park, I. J.; Lee, Y. K. Genistein, EGCG, and capsaicin inhibit adipocyte differentiation process via activating AMP-activated protein kinase. *Biochem. Biophys. Res. Commun.* **2005**, *338*, 694–699.

(31) Liu, M.; Wu, K.; Mao, X. G.; Wu, Y.; Ouyang, J. P. Astragalus polysaccharide improves insulin sensitivity in KKAY mice: regulation of PKB/GLUT4 signaling in skeletal muscle. *J. Ethnopharmacol.* **2010**, *127*, 32–37.

(32) Wang, J. L.; Zhang, J.; Zhao, B. T.; Wu, Y. Q.; Wang, C. X.; Wang, Y. P. Structural features and hypoglycaemic effects of *Cynomorium songaricum* polysaccharides on STZ-induced rats. *Food Chem.* **2010**, *120*, 443–451.

(33) Videla, L. A. Oxidative stress signaling underlying liver disease and hepatoprotective mechanisms. *World J. Hepatol.* **2009**, *1*, 72–78.

(34) Liu, Y. F.; Herschkovitz, A.; Boura-Halfon, S.; Ronen, D. Serine phosphorylation proximal to its phosphotyrosine binding domain inhibits insulin receptor substrate 1 function and promotes insulin resistance. *Mol. Cell. Biol.* **2004**, *24*, 9668–9681.